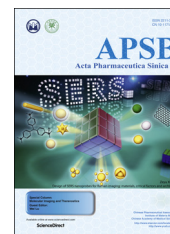




Chinese Pharmaceutical Association
Institute of Materia Medica, Chinese Academy of Medical Sciences

Acta Pharmaceutica Sinica B

www.elsevier.com/locate/apsb
www.sciencedirect.com



SHORT COMMUNICATION

A novel nitroreductase-enhanced MRI contrast agent and its potential application in bacterial imaging



Yun Liu^{a,b}, Leilei Zhang^{c,d,*}, Marc Nazare^e, Qingqiang Yao^{b,**},
Hai-Yu Hu^{c,d,*}

^aSchool of Medicine and Life Sciences, University of Jinan-Shandong Academy of Medical Sciences, Jinan 250200, China

^bInstitute of Materia Medica, Shandong Academy of Medical Sciences, Key Laboratory for Biotech-Drugs Ministry of Health, Key Laboratory for Rare & Uncommon Diseases of Shandong Province, Jinan 250062, China

^cState Key Laboratory of Bioactive Substances and Function of Natural Medicine, Institute of Materia Medica, Peking Union Medical College and Chinese Academy of Medical Sciences, Beijing 100050, China

^dBeijing Key Laboratory of Active Substances Discovery and Drugability Evaluation, Institute of Materia Medica, Peking Union Medical College and Chinese Academy of Medical Sciences, Beijing 100050, China

^eLeibniz-Forschungsinstitut für Molekulare Pharmakologie (FMP), Campus Berlin-Buch, Berlin 13125, Germany

Received 8 August 2017; received in revised form 1 October 2017; accepted 18 October 2017

KEY WORDS

Nitroreductase;
MRI contrast agent;
Smart imaging probes;
Bacterial imaging;
Bacterial infection

Abstract Nitroreductases (NTRs) are known to be able to metabolize nitro-substituted compounds in the presence of reduced nicotinamide adenine dinucleotide (NADH) as an electron donor. NTRs are present in a wide range of bacterial genera and, to a lesser extent, in eukaryotes hypoxic tumour cells and tumorous tissues, which makes it an appropriate biomarker for an imaging target to detect the hypoxic status of cancer cells and potential bacterial infections. To evaluate the specific activation level of NTR, great efforts have been devoted to the development of fluorescent probes to detect NTR activities using fluorogenic methods to probe its behaviour in a cellular context; however, NTR-responsive MRI contrast agents are still by far underexplored. In this study, *para*-nitrobenzyl substituted T_1 -weighted magnetic resonance imaging (MRI) contrast agent Gd-DOTA-PNB (probe **1**) has been designed and explored for the possible detection of NTR. Our experimental results show that probe **1** could serve as an MRI-enhanced contrast agent for monitoring NTR activity. The *in vitro* response and mechanism of the NTR catalysed reduction of probe **1** have been investigated through LC-MS and MRI. *Para*-nitrobenzyl substituted probe **1** was catalytically reduced by NTR to the intermediate *para*-aminobenzyl substituted probe which then underwent a rearrangement

*Corresponding authors at State Key Laboratory of Bioactive Substances and Function of Natural Medicine, Institute of Materia Medica, Peking Union Medical College and Chinese Academy of Medical Sciences, Beijing 100050, China.

**Corresponding author.

E-mail addresses: zhangleilei@imm.ac.cn (Leilei Zhang), yao_jmm@163.com (Qingqiang Yao), haiyu.hu@imm.ac.cn (Hai-Yu Hu).

Peer review under responsibility of Institute of Materia Medica, Chinese Academy of Medical Sciences and Chinese Pharmaceutical Association.

<https://doi.org/10.1016/j.apsb.2017.11.001>

2211-3835 © 2018 Chinese Pharmaceutical Association and Institute of Materia Medica, Chinese Academy of Medical Sciences. Production and hosting by Elsevier B.V. This is an open access article under the CC BY-NC-ND license (<http://creativecommons.org/licenses/by-nc-nd/4.0/>).

elimination reaction to Gd-DOTA, generating the enhanced T_1 -weighted MR imaging. Further, LC-MS and MRI studies of living *Escherichia coli* have confirmed the NTR activity detection ability of probe **1** at a cellular level. This method may potentially be used for the diagnosis of bacterial infections.

© 2018 Chinese Pharmaceutical Association and Institute of Materia Medica, Chinese Academy of Medical Sciences. Production and hosting by Elsevier B.V. This is an open access article under the CC BY-NC-ND license (<http://creativecommons.org/licenses/by-nc-nd/4.0/>).

1. Introduction

Molecular imaging provides a sensitive and specific method for non-invasive, real-time monitoring and visualization of biological processes *in vivo*^{1–4}. Magnetic resonance imaging (MRI) has several advantages over other clinical diagnostic techniques for molecular imaging, in virtue of its high spatial resolution, unlimited penetration depth, and lack of harmful radiation^{5–7}. Over the past three decades, paramagnetic Gd(III) complexes have been widely developed as contrast agents to dramatically improve detection sensitivity and specificity of MRI by shortening the relaxation times of the surrounding water proton resulting in an enhanced imaging contrast^{8–11}. At present, the contrast agents most commonly used in clinical MRI are mainly small molecule gadolinium chelates, such as Magnevist (Gd-DTPA), Dotarem (Gd-DOTA), ProHance (Gd-HP-DO3A), etc. To further improve the enhancing effects and detect physiological changes at the molecular level, the smart MRI contrast agents have been developed and used^{12–15}. These probes are capable of monitoring physiological processes by changing signal properties with changes in the physiological environment, such as enzyme^{16–20}, metal ion concentration^{20–23}, pH value^{24,25}, temperature²⁶, etc. Recently, applications of enzyme-activatable MRI contrast agents have been reported.

Nitroreductases (NTRs), are a family of flavin-containing enzymes widely exists in bacteria, which can effectively catalyze the reduction of nitroaromatic compounds into hydroxylamines or amines in the presence of reduced nicotinamide adenine dinucleotide (NADH) or nicotinamide adenine dinucleotide phosphate (NADPH) as a cofactor *via* an one-electron reduction pathway^{27–31}. An increasing number of nitroaromatic compounds have proved to be superior substrates for NTRs opening up the opportunity to develop enzyme-activatable probes, which is, given the role of the NTRs of great significance for environmental and human health^{32–34}. Great effort has been devoted to the design of activatable optical probes for sensing NTR activities within hypoxic tumor cells; lately, optical probes for detecting NTR activities in bacterial lysates have been developed as well^{33–38}. In comparison, a few NTR-activatable MRI contrast agents have been developed^{39,40}, and there appears to have been no real time NTR enzymatic activity detection in bacteria using an MRI method.

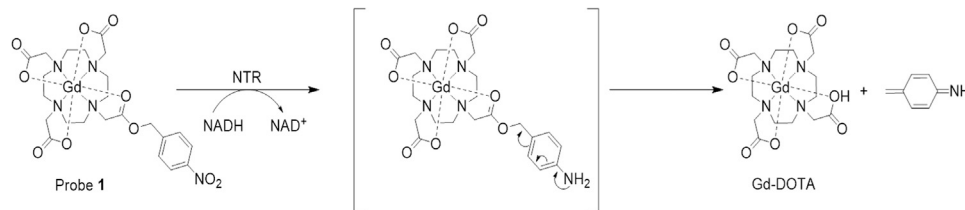
In this study, we designed and synthesized a novel NTR-enhanced MRI contrast agent: Gd-DOTA-PNB (probe **1**) by conjugating Gd-

DOTA with an NTR-sensing moiety, a *p*-nitrobenzyl group. Probe **1** has been characterized by ¹H NMR, ¹³C NMR, MS and evaluated as a new NTR-enhanced MRI contrast agent, which may potentially be used for the diagnosis of bacterial infections. Conceptually, we hypothesized that the *p*-nitrobenzyl moiety (PNB) of probe **1** would be reduced to a primary aromatic amino group by NTR in the presence of NADH, which would then trigger a self-immolative fragmentation through a rearrangement elimination reaction and formation of Gd-DOTA (Scheme 1) resulting a relaxivity enhancement, which could be used for NTR activities detection. The *in vitro* response and mechanism of the NTR catalysed reduction of probe **1** have been investigated through LC-MS and MRI. Further, LC-MS and MRI studies of living *Escherichia coli* (*E. coli*) have confirmed the NTR activity detection ability of probe **1** at a cellular level, which hint to the potential application of probe **1** for the diagnosis of bacterial infections.

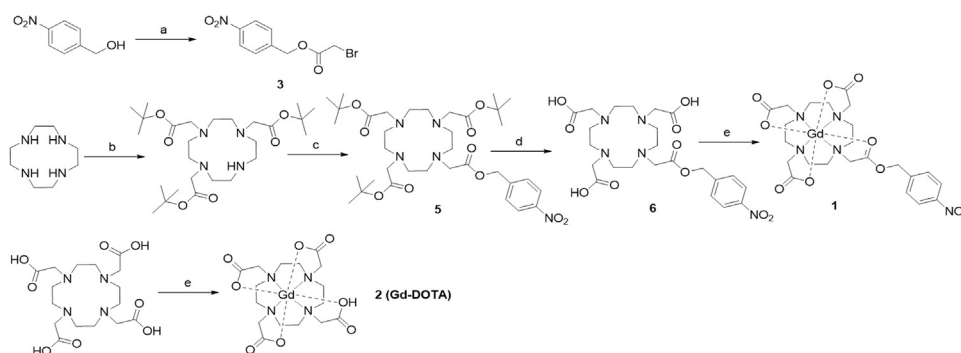
2. Materials and methods

2.1. General methods

All chemicals were purchased from J&K (Beijing, China). Commercially available reagents were used without further purification. Unless otherwise noted, all reactions were performed under a nitrogen or argon atmosphere. NTR (≥ 100 units/mg) from *E. coli*, and NADH were purchased from Sigma-Aldrich (Shanghai, China). The lyophilized powder of NTR was dissolved in pure water, and the solution was divided into aliquots suitable for daily experiments. All these enzyme solutions were stored at -20 °C and allowed to thaw before use according to the reported procedure, under the premise of no change of the enzyme activity^{33,34}. A stock solution (10 mmol/L) for compounds **1** and **2** were prepared by dissolving an appropriate amount of them in H₂O. The *E. coli* (ATCC 25922) was purchased from American Type Culture Collection (ATCC), USA. MTS (3-(4,5-dimethylthiazol-2-yl)-5-(3-carboxymethoxyphenyl)-2-(4-sulfo-phenyl)-2H-tetrazolium, inner salt) was obtained from Promega (Beijing, China). OD values and MTS assays were also measured by TECAN Spark 10 M microplate reader (Männedorf, Switzerland). Thin layer chromatography (TLC) was carried out with Silica Gel 60 F254, and column chromatography with silica gel (200–300 mesh). All ¹H NMR spectra were recorded at 600 MHz



Scheme 1 Structure and reaction response mechanism of probe **1** to NTR.



Scheme 2 Synthesis of probe **1**. (a) bromoacetyl bromide, DMAP, toluene, 92%. (b) *t*-Butyl bromoacetate, sodium acetate, DMA, 62%. (c) Compound **3**, K_2CO_3 , MeCN, 89%. (d) TFA/ triethylsilane/ H_2O , 0 °C, 63%. (e) $GdCl_3 \cdot 6H_2O$, NaOH, pH 6.5–7.0, 61%.

and ^{13}C NMR spectra were recorded at 150 MHz respectively (Varian VNS, 600 MHz, USA). Mass spectra (MS) were measured with an Exactive Plus Orbitrap mass spectrometer via an ESI interface (ThermoFisher Scientific, Bremen, Germany). Characterization of MR properties were measured at a Pharmscan 70/16 USmagnetic resonance imaging scanner (Bruker, Switzerland) fitted with RF RES 300 1H 089/072 QSN TR AD volume coil.

2.2. Analysis and determination of the conversion kinetics by LC–MS

To investigate the kinetics of the NTR-catalyzed reaction of probe **1**, the conversion reaction mixture containing probe **1** (200 μ mol/L), NTR (30 μ g/mL) and NADH (500 μ mol/L) at 37 °C in 0.9% aqueous NaCl solution was analyzed. The reaction was performed in a 0.5 mL eppendorf tube with a reaction volume of 50 μ L at different time points (0, 3, 6, 12 and 24 h) and quenched by addition of acetonitrile (60 μ L). After centrifugation at 6500 rpm for 3 min (HC-2062 High speed centrifuge, Anhui USTC Zonkia Scientific Instruments Co., Ltd., Hefei, China), the supernatants were analyzed by LC–MS. The conversion rate of **1** to Gd-DOTA (**2**) following the enzymatic reaction was calculated according to the percentage of peak area of **1**. Pseudo-first-order rate constants for enzymatic hydrolysis were determined based on the equation $y = A_0 \times e^{-k_{obs}t}$ (where $A_0 = 1$ and $t^{-1} = k_{obs}$), using GraphPad Prism 5 (GraphPad Software Inc., USA).

2.3. Determination of the enzymatic reaction in vitro by an HPLC assay

The specific enzymatic reaction of probe **1** to NTR was conducted in 0.9% aqueous NaCl solution. Four aqueous solutions were prepared: (A) 200 μ mol/L probe **1** and 500 μ mol/L NADH in 0.9% aqueous NaCl solution; (B) 200 μ mol/L probe **1**, 500 μ mol/L NADH, and 30 μ g/mL NTR in 0.9% aqueous NaCl solution; (C) 200 μ mol/L probe **1**, 500 μ mol/L NADH, 30 μ g/mL NTR and 0.25 mmol/L dicoumarin in 0.9% aqueous NaCl solution; (D) 200 μ mol/L probe **1**, 500 μ mol/L NADH, 30 μ g/mL NTR and 0.5 mmol/L dicoumarin in 0.9% aqueous NaCl solution. Reactions were performed for 6 h at 37 °C, and quenched by adding CH_3CN (250 μ L). Then, after centrifugation the supernatants (6500 rpm, 3 min) were measured by high performance liquid chromatography (HPLC) equipped with an evaporative light scattering detector (ELSD). The HPLC method was as follows: mobile phase A was acetonitrile with 0.1% trifluoroacetic acid, and mobile phase B consisted of water with 0.1% trifluoroacetic acid; a

linear gradient was set from 1% to 5% B in 10 min, followed by a gradient to 90% B in 10 min, then at 90% B for 2 min; the flow rate was 1.0 mL/min, and 50 μ L of sample was injected. The conversion rate of **1** to Gd-DOTA following the enzymatic reaction was calculated according to the percentage of peak area of **1** before incubation.

2.4. Bacteria and cell culture

E. coli (ATCC 25922) was used in this study. The Luria-Bertani (LB) culture medium was prepared by dissolving 10 g bacto-tryptone, 5 g bactoyeast extract and 5 g NaCl in 1 L water. The culture medium was autoclaved prior to use. For determining the NTR activity generated by *E. coli*, single colony from the stock agar plate was added to 20 mL of LB culture media, which then was grown at 37 °C on a shaker incubator (180 rpm, THZ-C-1, Suzhou, China) overnight followed by a subculture until an OD_{600} of approximately 5–7 was reached. The Raw 264.7 cells, 293 A cells, rat fibroblast L6 cells and HepG2 cells were cultured in Dulbecco's modified Eagle's medium (DMEM) with 10% fetal bovine serum (FBS) under humidified atmosphere of 5% CO_2 at 37 °C.

2.5. In vitro LC–MS/ELSD measurement of the conversion and selectivity of probe **1** incubated with bacteria

E. coli cells were cultured for 12 h in LB culture media at 37 °C. Bacterial strains cultured overnight was harvested and washed three times with 0.9% aqueous NaCl solution. The washed cells were resuspended in 0.9% aqueous NaCl solution with an OD_{600} of 5–7 and were divided into 500 μ L aliquots. The following samples were set up: (A) probe **1** (200 μ mol/L) only, (B) cells treated with probe **1** (200 μ mol/L), (C) cells treated with probe **1** (200 μ mol/L) and dicoumarin (0.5 mmol/L). After incubation at 37 °C for 24 h, 500 μ L CH_3OH were added and the samples subjected to subsequent ultrasonication using an ultrasonic cell disintegrator (SONIC-VCX-130, USA). Then after centrifugation (6500 rpm, 3 min) the supernatants were measured by HPLC–ESI-MS and HPLC–ELSD analyses.

2.6. Longitudinal relaxation time (T_1) measurement

The longitudinal relaxation time (T_1) of the Gd(III) complexes in different solutions was measured using the standard inversion recovery spin-echo sequence on 7 T scanner operating at 300 MHz and room temperature (Pharmscan 70/16 US, Bruker, Switzerland). For acquisition of T_1 relaxation time, a T_1 map rapid-

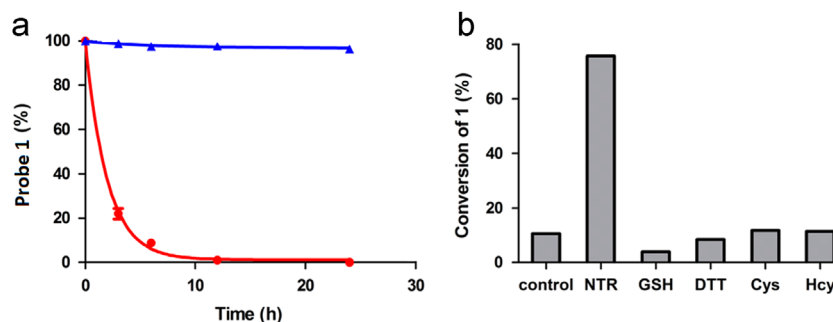


Figure 1 (a) Plot of reduction of probe **1** with (red) or without (blue) NTR at 37 °C (in 0.9% aqueous NaCl solution) monitored by LC–MS. Individual data points represent the integration of the peak area of probe **1** post-incubation with or without NTR divided by the peak area of probe **1** before incubation (multiplied by 100 to give percent complex hydrolysis). The red line corresponds to a pseudo first-order kinetic fit of the data with a half-life of $t_{1/2}=2.56$ h for **1**. Data are mean \pm SD ($n=2$). (b) Conversion of **1** (200 $\mu\text{mol/L}$) to various species: control (probe **1**), NTR (30 $\mu\text{g/mL}$), GSH (1 mmol/L), DTT (1 mmol/L), Cys (1 mmol/L), Hcy (1 mmol/L).

acquisition refocused echo (T_1 map RARE) pulse sequence was used. The following parameter values were utilized: static echo time = 8 ms, variable repetition time = 200, 400, 800, 1500, 3000, and 5500 ms, field of view = 50×50 mm², matrix size = 256×192 , number of axial slices = 1, slice thickness = 1.0 mm, and averages = 1. Paravision 6.0 software (Bruker) was used for T_1 analysis, by mono-exponential curve-fitting of image intensities of selected regions of interest (ROIs) from the axial slice.

2.7. Characterization of the MR properties in vitro

To determine relaxivity (r_1) of probe **1** and Gd-DOTA in different solutions, a 10 mmol/L stock solution of either probe **1** or Gd-DOTA in the appropriate buffer was diluted to give 500 μL of each of seven concentrations for each run: 0, 0.1, 0.2, 0.4, 0.6, 0.8, and 1.0 mmol/L. The values of r_1 ($\text{mM}^{-1} \text{s}^{-1}$) were determined from the slope of the linear fit of the relaxation rate ($1/T_1, \text{s}^{-1}$) plotted against the compound concentration (mmol/L). All lines were fitting with $R^2 > 0.997$.

To study the effect of the NTR reduction on the T_1 value of probe **1**, NTR was dissolved in water to form an aqueous solution. For the T_1 measurements of probe **1** in the presence or absence of NTR and NADH, the follow reactions were set up: (a) 200 $\mu\text{mol/L}$ probe **1** in 0.9% aqueous NaCl solution; (b) 200 $\mu\text{mol/L}$ probe **1** and 500 $\mu\text{mol/L}$ NADH in 0.9% aqueous NaCl solution; (c) 200 $\mu\text{mol/L}$ probe **1**, 500 $\mu\text{mol/L}$ NADH, and 30 $\mu\text{g/mL}$ NTR in 0.9% aqueous NaCl solution. The T_1 of these solutions were measured after incubation for 12 h at 37 °C.

2.8. In vitro MR imaging of *E. coli* treated with probe **1**

E. coli cells were cultured for 12 h in LB culture media at 37 °C. Bacterial strains cultured overnight were harvested and washed three times with 0.9% aqueous NaCl solution. The washed cells were resuspended in 0.9% aqueous NaCl solution until an OD₆₀₀ of 6 was reached. Then 500 μL aliquots (5.1×10^9 CFU/mL) were (A) untreated, (B) treated with 200 $\mu\text{mol/L}$ of probe **1** for 0 h and (C) treated with 200 $\mu\text{mol/L}$ of probe **1** for 24 h. After incubation at 37 °C for 24 h, the samples were imaged using a RF RES 300 1 H 089/072 QSN TR AD volume coil (Pharmscan 70/16 US, Bruker, Switzerland). For acquisition of T_1 relaxation times, a T_1 map rapid acquisition with refocused echoes (T_1 map RARE) pulse sequence was used. For T_1 -weighting, the following parameters were used: TR = 400 ms, TE = 8 ms, flip angle = 90°, NEX = 1,

FOV = 55×55 mm², slice thickness = 1 mm, and matrix size = 256×192 .

2.9. Cytotoxicity assays

The cytotoxicity of probe **1** was evaluated following the approach reported previously.³ The Raw 264.7 cells, 293 A cells, rat fibroblast L6 cells and HepG2 cells were seeded on a 96-wells containing 7500 cells per well in 100 μL DMEM media and incubated for overnight before adding probe **1**. Upon incubation with different concentration of probe **1** at 37 °C for 48 h, then incubated with cell culture medium containing 20% MTS per well. After 3 h of incubation at 37 °C, the absorbance was measured at 490 nm using a TECAN Spark 10 M microplate reader. Cell viabilities at various concentrations are given as a percentage of control sample without probe. Each experiment was repeated three times. The cell survival rate from the control group was considered to be 100%.

3. Results and discussion

3.1. Synthesis of the Gd(III) complexes

The Gd(III) complexes of probe **1** and Gd-DOTA (**2**) were synthesized as shown in Scheme 2. 2-(4-Nitrobenzyl)-bromoacetate (**3**) was synthesized via alkylation-coupling reactions between 4-Nitrobenzyl alcohol and bromoacetyl bromide in the presence of DMAP and toluene in 92% yield without further purification. The bromoacetyl group was used as a linker to connect the DO3A-tris-tert-butyl ester (**4**) and 4-nitrobenzyl alcohol. Subsequently, the *tert*-butyl groups in DOTA were removed with TFA/trimethylsilane/H₂O (98:1:1) to obtain DOTA-PNB (**6**). The ligand, DOTA-PNB (**6**), was characterized by ESI-MS and NMR, and its purity was determined by HPLC to be greater than 98% (Supplementary information Fig. S1). Finally, the ligands DOTA-PNB and DOTA were reacted with GdCl₃·6H₂O in water at pH 6.5–7.0 to give Gd-DOTA-PNB (probe **1**) and Gd-DOTA, respectively. Probe **1** was obtained in 61% yield, while Gd-DOTA was obtained in 13% yield due to the lack of a chromophore on Gd-DOTA for spectrometric detection which was hampering the experimental isolation procedure.

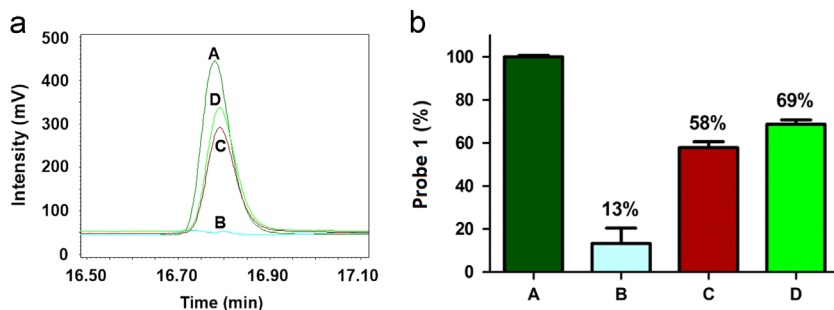


Figure 2 (a) HPLC traces of different reaction systems. (A): 200 μmol/L probe **1** and 500 μmol/L NADH in 0.9% aqueous NaCl solution (control); (B): system (A) + 30 μg/mL NTR; (C): system (B) + 0.25 mmol/L dicoumarin; (D): system (B) + 0.5 mmol/L dicoumarin. All the reactions were performed at 37 °C for 6 h. (b) The percentage of probe **1** in different reaction systems A, B, C, D. The control (A) was considered to be 100%. Data are mean ± SD ($n=3$).

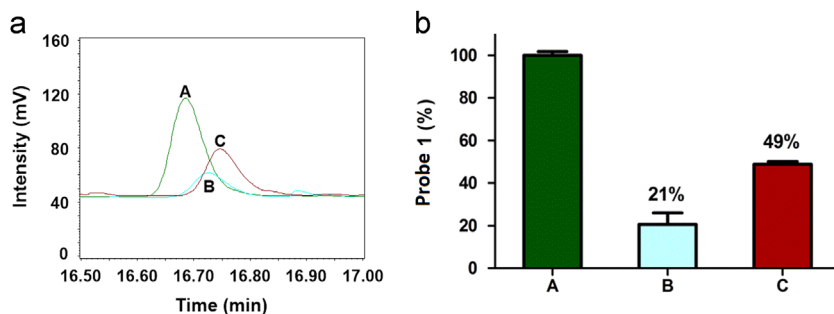


Figure 3 (a) HPLC traces of different reaction systems. (A): probe **1** (200 μmol/L) in 0.9% aqueous NaCl solution (control); (B): system (A) + *E. coli* (OD₆₀₀=6.2); (C): system (B) + dicoumarin (0.5 mmol/L). All the reactions were performed at 37 °C for 24 h. (b) The percentage of probe **1** in different reaction systems A, B, C. The control (A) was considered to be 100%. Data are means ± SD ($n=3$).

3.2. Activation mechanism and enzyme kinetics

LC-MS is a convenient and practical method to detect and identify the products of enzyme-catalyzed reaction^{41,42}. To monitor the ability of the NTR to activate the probe **1**, the reaction mixture was analyzed by LC-MS after incubating probe **1** (200 μmol/L) with NTR (30 μg/mL) and NADH (500 μmol/L) at 37 °C in 0.9% aqueous NaCl solution (Supplementary Information Fig. S2). Probe **1** and its product Gd-DOTA are readily discriminated by their appropriate positive mode ESI-MS, and through spiking with authentic compound. The ESI-MS spectrum of the reaction solution definitely displays the presence of Gd-DOTA as a major product at 3.77 min ($m/z=559.10$, $[M+H]^+$). Unreacted probe **1** decreased markedly at 19.76 min ($m/z=695.14$, $[M+H]^+$) after 3 h, which was disappeared after 24 h (Supplementary information Figs. S2–3). Moreover, the kinetics of NTR reaction were investigated by following the decrease of probe **1** post-incubation with NTR at 37 °C in 0.9% aqueous NaCl solution (Fig. 1a). After 20 h, 99.5% of **1** was hydrolyzed resulting in a rate constant of $7.52 \times 10^{-5} \text{ s}^{-1}$ (k_{obs} , 37 °C) by assuming a pseudo first-order kinetics. This rate constant corresponds to a half-life of $t_{1/2}=2.56$ h. Therefore, all these data indicate that the reaction most likely undergoes the proposed reduction-elimination mechanism as shown in Scheme 1. Considering the complexity of the intracellular environment, the interferences of various biothiols (GSH, DTT, cysteine and homocysteine) were studied. As shown in Fig. 1b, the probe shows high selectivity for NTR over the other species tested, even including reductive biothiols at a high concentration, which may be ascribed to the specific reduction of the substrate (*p*-nitrobenzyl) by the enzyme.

3.3. In vitro HPLC assay of enzymatic reaction

Having established the activation mechanism of probe **1**, we then evaluated whether probe **1** is specific for NTR. To study the selectivity of probe **1** for NTR, the effect of the known competitive inhibitor dicoumarin^{33,36} of NTR on the activity of the enzyme was examined using high performance liquid chromatography (HPLC) equipped with an evaporative light scattering detector (ELSD) (Fig. 2 and Supplementary information Fig. S4). As shown in Fig. 2a, HPLC chromatograms of probe **1** (200 μmol/L) incubated with NADH (500 μmol/L), NTR (30 μg/mL), and the NTR inhibitor dicoumarin (0.25/0.5 mmol/L) for 6 h at 37 °C in 0.9% aqueous NaCl solution were monitored. On incubation with NTR in reaction system, probe **1** ($t_R=16.8$ min) was efficiently

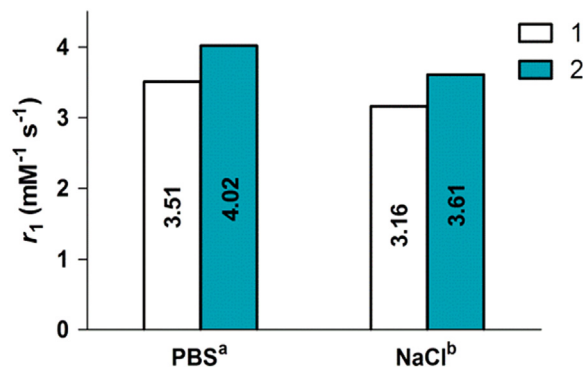


Figure 4 T_1 relaxivity of probe **1** (1) and Gd-DOTA (2) at 300 MHz, r.t., ^a10 mmol/L PBS, pH=5.35; ^b0.9% aqueous NaCl solution.

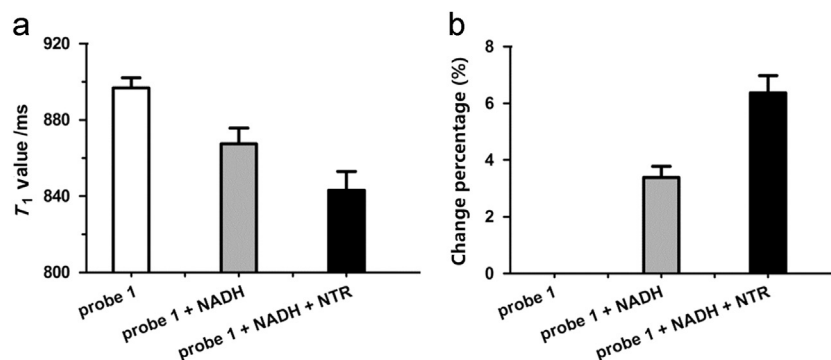


Figure 5 MR studies with probe **1** upon activation with NTR *in vitro*. (a) T_1 value reduction of probe **1** (200 $\mu\text{mol/L}$) in the presence of NADH (500 $\mu\text{mol/L}$) and NTR (30 $\mu\text{g/mL}$) in 0.9% aqueous NaCl solution at 37 $^\circ\text{C}$. (b) Change percentage in R_1 ($1/T_1$) of NTR-catalyzed hydrolysis of probe **1**. T_1 value was measured with a Pharmscan 70/16 US (Bruker, Switzerland) imaging scanner at r.t., using the standard inversion recovery program. Data represent mean value \pm SD, $n=2$.

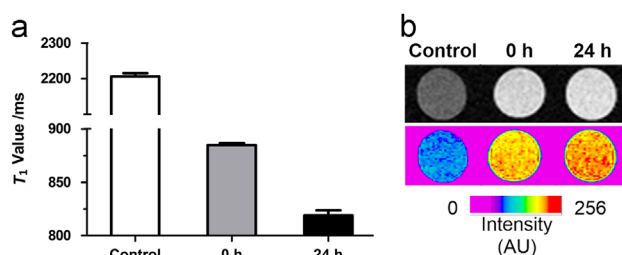


Figure 6 Cellular MR studies of incubating with probe **1**. (a) T_1 values (7 T) of *E. coli* cell pellets after incubation with 200 $\mu\text{mol/L}$ of probe **1** for 0 or 24 h. (b) T_1 -weighted MR images (7 T, TE/TR=8/400 ms) of *E. coli* cell pellets after incubation with 200 $\mu\text{mol/L}$ of probe **1** for 0 h or 24 h. Data are means \pm SD ($n=3$).

converted into Gd-DOTA (the same t_R as NADH) and nearly completely reduced after 6 h. In contrast, residual content probe **1** in the presence of 0.25 mmol/L dicoumarin (curve/bar graph C) indicated by the peak area is much larger than the content of **1** (curve/bar graph B) in the absence of the inhibitor after 6 h. Higher concentration of dicoumarin (0.5 mmol/L) resulted increased remaining probe **1** content after 6 h (curve/ bar graph D) roughly equally to the control reaction without NTR (incubation of probe **1** with only NADH, curve/ bar graph A, Fig. 2b). We conclude that the NTR activity can be effectively inhibited by dicoumarin, and thus the reduction of probe **1** to NTR is indeed attributed to the enzyme catalyzed cleavage reaction, confirming the good selectivity of probe **1** for NTR detection.

3.4. *In vitro* LC-MS/ELSD assay of probe **1** incubated with bacteria

It is known that *E. coli* can generate NTR, and this bacterial enzyme has been considered to be useful for the removal of nitroaromatic pollutants^{27,28,30,43}. To study whether the probe **1** could detect microbial NTR activity at a cellular level, we measured the time dependent conversion of probe **1** (200 $\mu\text{mol/L}$) in *E. coli* for 24 h by HPLC chromatograms and ESI-MS spectra (Fig. 3 and Supplementary Information Fig. S5). Fig. 3a shows HPLC chromatograms of probe **1** at 16.7 min, which indicates that the peak area of probe **1** after incubating with *E. coli* (curve/bar graph B) is less than that (curve/bar graph A) in the absence of the bacteria, while addition of dicoumarin (0.5 mmol/L) to the bacterial culture before treatment with the probe **1** (curve/bar graph C) significantly decrease the

reduction rate of probe. By calculating percentage of probe **1**, we discover that probe **1** is reduced about 80% after incubating with *E. coli*, and decreasing to about 50% by the addition of the NTR inhibitor dicoumarin (Fig. 3b). Moreover, the ESI-MS spectrum of probe **1** under the above conditions is shown in Supplementary Information Fig. S5. Here, the peak area change of probe **1** in the MS spectrum is consistent with the peak area change of Fig. 3. This result shows that probe **1** can be reduced by NTR of *E. coli* and the reduction can be inhibited by the NTR inhibitor dicoumarin, demonstrating the activation specificity of the probe **1** towards NTR. Taken together, this suggest that probe **1** may be used as a microbial growth indicator.

3.5. Relaxometric studies of the Gd(III) complexes *in vitro*

The efficiency of MR contrast agent is defined according to the parameter relaxivity (r_1), which is a weigh of the extent to which the paramagnetic compound (per concentration unit), shortens the longitudinal relaxation time (T_1) of water protons.⁵ To study relaxometric properties of the probe, the longitudinal relaxivity (r_1) values of probe **1** and the predicted reduction product, Gd-DOTA (**2**), are determined at 7 T, 300 MHz and room temperature (Fig. 4 and Supplementary information Fig. S6). As shown in Fig. 4, the r_1 value of Gd-DOTA in PBS buffer (pH = 5.35) is 4.02 $\text{mM}^{-1} \text{s}^{-1}$, which is 15% higher than that of **1** (3.51 $\text{mM}^{-1} \text{s}^{-1}$). Owing to enzyme reaction in 0.9% aqueous NaCl solution, the relaxivities of probe **1** and Gd-DOTA were also determined under these conditions. Here, the relaxivities of probe **1** and Gd-DOTA were 3.16 $\text{mM}^{-1} \text{s}^{-1}$ and 3.61 $\text{mM}^{-1} \text{s}^{-1}$ respectively, which are lower than observed in

PBS buffer but show the same trend with a 14% rise in relaxivity from probe **1** to Gd-DOTA. In this case, the phosphate could coordinate to DO3A analogues in a monodentate fashion^{17,44,45} and compete with intramolecular coordination, then increase the number of water molecules coordinated to the metal center. Therefore, the relaxivities in PBS buffer are expected to be higher than that in 0.9% aqueous NaCl solution. In addition, the difference in r_1 relaxivity between probe **1** and Gd-DOTA can provide the evidence for study of MRI contrast agent probe **1** reduced by NTR.

To evaluate probe **1** as a potential NTR-responsive MRI contrast agent, probe **1** (200 $\mu\text{mol/L}$) was incubated with NADH (500 $\mu\text{mol/L}$) and NTR (30 $\mu\text{g/mL}$) at 37 °C for 12 h in 0.9% aqueous NaCl solution and the change in the longitudinal relaxation time (T_1) was evaluated. We observed that the T_1 value of probe **1** is 897 ± 5 ms, while the T_1 is 843 ± 9 ms decreased by 6% in the presence of NTR, which is consistent with the relaxometric study (Fig. 5). The changes in T_1 values can be explained the significant increase of product **2** (Gd-DOTA) upon enzymatic cleavage of probe **1** over time after NTR treatment, resulting in a decrease in the longitudinal relaxation time (T_1). We conclude that probe **1** can therefore selectively respond to NTR and detect its activity in an MRI setting. Moreover, under optimized conditions (reaction at 37 °C for 6 h in 0.9% aqueous NaCl solution in the presence of 500 $\mu\text{mol/L}$ NADH), the T_1 values of probe **1** (200 $\mu\text{mol/L}$) to NTR at different concentrations is shown in Supplementary Information Fig. S7a. As can be seen, a gradual decrease in T_1 value is observed with increase in the NTR concentrations, and a good linearity is obtained in the range of 5 to 40 $\mu\text{g/mL}$ (Supplementary Information Fig. S7b), with the regression equation $T_1 = -1.0474 \times [c] \mu\text{g/mL} + 894.82$ ($R^2 = 0.9926$). The detection limit is determined to be 24 ng/mL NTR.

3.6. *In vitro* MR imaging of *E. coli* treated with probe **1**

In addition, MR imaging was performed to evaluate the efficiency of probe **1** for detecting endogenous NTR activity in *E. coli*. The experiments were carried out at 7 T using three incubations: (A) bacteria alone, (B) bacteria+probe **1**, incubated for 0 h, (C) bacteria+probe **1**, incubated for 24 h. As shown in Fig. 6a, the T_1 value of *E. coli* after incubation with **1** (200 $\mu\text{mol/L}$) for 24 h is 819 ± 5 ms reduced by 8% as compared to 0 h (885 ± 2 ms). The shorter T_1 value was again consistent with the results of the T_1 -weighted images of bacteria shown in Fig. 6b, where *E. coli* after incubation with **1** for 24 h manifested higher MR signal intensity than at 0 h. The results of *in vitro* MR imaging studies of *E. coli* treated with probe **1** indicated that probe **1** could permeate *E. coli* cell membrane and be subsequently activated by the NTR, leading to an enhanced MRI contrast. Our experimental results show that probe **1** could serve as an MRI-enhanced contrast agent for monitoring NTR activity in living bacteria. Considering NTRs are also present in eukaryotes hypoxic tumour cells, MR imaging hypoxia was performed in Hela cells by probe **1**. In this experiment, Hela cells (1×10^6) were incubated with 200 $\mu\text{mol/L}$ probe **1** under hypoxic conditions (1% pO_2) at 37 °C for 0 h or 24 h. As shown in Supplementary Information Fig. S8, Hela cells treated with probe **1** for 24 h show shorter T_1 value (858 ± 8 ms) by 6% than 0 h (914 ± 2 ms), which are not as obvious as that in *E. coli*.

3.7. Cytotoxicity of probe **1**

Finally, we evaluated the cytotoxicity of probe **1** using standard MTS assays to further qualify our probe for *in vivo* studies and

exclude any detrimental interfering effects in our cellular studies. As shown in Supplementary Information Fig. S9, after incubation with probe **1** for 48 h, the viability of the cells showed no significant change, and approximately 80% of cells survived even at the very high concentration of 500 $\mu\text{mol/L}$ of probe **1**. The results indicate that our probe **1** has a low cytotoxicity and good biocompatibility.

4. Conclusions

In conclusion, we have designed and synthesized an NTR-enhanced MRI contrast agent, probe **1**, which is convenient for the detection of NTR activity *in vitro* and in living *E. coli*. The *para*-nitrobenzyl moiety of probe **1** can be selectively reduced by NTR in the presence of NADH, followed by a self-immolative fragmentation, and formation of the Gd-DOTA, which was confirmed by LC-MS and HPLC analyses. Furthermore, relaxometric measurements revealed that the longitudinal T_1 relaxivity of probe **1** is different from Gd-DOTA and thus changes in concentration of both species are detectable by MRI. The longitudinal relaxation time (T_1) was decreased by 6% in response to NTR. More importantly, MR images studies of living *E. coli* incubated with probe **1** resulted an 8% signal intensity enhancement, which indicates that probe **1** could serve as an MRI-enhanced contrast agent for monitoring NTR activity. Probe **1** is the first reported smart MRI contrast agents for monitoring NTR activity in living bacteria, which has the potential for a wider application in therapeutic NTR-activated prodrug treatment in clinical research.

Acknowledgments

This study is supported by Sino-German research project GZ 1271, Peking Union Medical College (PUMC) Youth Fund (No. 3332016056) and the Innovation Project of Shandong Academy of Medical Sciences.

Appendix A. Supporting information

Supplementary data associated with this article can be found in the online version at [doi:10.1016/j.apsb.2017.11.001](https://doi.org/10.1016/j.apsb.2017.11.001).

References

1. Hu HY, Gehrig S, Reither G, Subramanian D, Mall MA, Plettenburg O, et al. FRET-based and other fluorescent proteinase probes. *Biotechnol J* 2014;9:266–81.
2. Hu HY, Vats D, Vizovisek M, Kramer L, Germanier C, Wendt KU, et al. *In vivo* imaging of mouse tumors by a lipidated cathepsin S substrate. *Angew Chem Int Ed* 2014;53:7669–73.
3. Zhang Q, Wang Q, Xu S, Zuo L, You X, Hu HY. Aminoglycoside-based novel probes for bacterial diagnostic and therapeutic applications. *Chem Commun* 2017;53:1366–9.
4. Ferreira K, Hu HY, Fetz V, Prochnow H, Rais B, Müller PP, et al. Multivalent siderophore-DOTAM conjugates as theranostics for imaging and treatment of bacterial infections. *Angew Chem Int Ed* 2017;56:8272–6.
5. Lauffer RB. Paramagnetic metal complexes as water proton relaxation agents for NMR imaging: theory and design. *Chem Rev* 1987;87:901–27.

- Pierre VC, Allen MJ, Caravan P. Contrast agents for MRI: 30+ years and where are we going?. *J Biol Inorg Chem* 2014;**19**:127–31.
- Verwilt P, Park S, Yoon B, Kim JS. Recent advances in Gd-chelate based bimodal optical/MRI contrast agents. *Chem Soc Rev* 2015;**44**:1791–806.
- Aime S, Botta M, Terreno E. Gd(III)-based contrast agents for MRI. *Adv Inorg Chem* 2005;**57**:173–237.
- Aime S, Castelli DD, Crich SG, Gianolio E, Terreno E. Pushing the sensitivity envelope of lanthanide-based magnetic resonance imaging (MRI) contrast agents for molecular imaging applications. *Acc Chem Res* 2009;**42**:822–31.
- Hu HY, Lim NH, Juretschke HP, Ding-Pfennigdorff D, Florian P, Kohlmann M, et al. *In vivo* visualization of osteoarthritic hypertrophic lesions. *Chem Sci* 2015;**6**:6256–61.
- Hu HY, Lim NH, Ding-Pfennigdorff D, Saas J, Wendt KU, Ritzler O, et al. DOTAM derivatives as active cartilage-targeting drug carriers for the treatment of osteoarthritis. *Bioconjugate Chem* 2015;**26**:383–8.
- Major JL, Meade TJ. Bioresponsive, cell-penetrating, and multimeric MR contrast agents. *Acc Chem Res* 2009;**42**:893–903.
- Davies GL, Kramberger I, Davis JJ. Environmentally responsive MRI contrast agents. *Chem Commun* 2013;**49**:9704–21.
- Heffern MC, Matosziuk LM, Meade TJ. Lanthanide probes for bioresponsive imaging. *Chem Rev* 2014;**114**:4496–539.
- Hingorani DV, Bernstein AS, Pagel MD. A review of responsive MRI contrast agents: 2005–2014. *Contrast Media Mol Imaging* 2015;**10**:245–65.
- Moat RA, Fraser SE, Meade TJ. A “smart” magnetic resonance imaging agent that reports on specific enzymatic activity. *Angew Chem Int Ed* 1997;**36**:726–8.
- Duimstra JA, Femia FJ, Meade TJ. A gadolinium chelate for detection of β -glucuronidase: a self-immolative approach. *J Am Chem Soc* 2005;**127**:12847–55.
- Chen SH, Kuo YT, Singh G, Cheng TL, Su YZ, Wang TP, et al. Development of a Gd(III)-based receptor-induced magnetization enhancement (RIME) contrast agent for β -glucuronidase activity profiling. *Inorg Chem* 2012;**51**:12426–35.
- Ye D, Shuhendler AJ, Pandit P, Brewer KD, Tee SS, Cui L, et al. Caspase-responsive smart gadolinium-based contrast agent for magnetic resonance imaging of drug-induced apoptosis. *Chem Sci* 2014;**5**:3845–52.
- MacRenaris KW, Ma Z, Krueger RL, Carney CE, Meade TJ. Cell-permeable esterase-activated Ca(II)-sensitive MRI contrast agent. *Bioconjugate Chem* 2016;**27**:465–73.
- Gündüz S, Nitta N, Vibhute S, Shibata S, Mayer ME, Logothetis NK, et al. Dendrimeric calcium-responsive MRI contrast agents with slow *in vivo* diffusion. *Chem Commun* 2015;**51**:2782–5.
- Xiao YM, Zhao GY, Fang XX, Zhao YX, Wang GH, Yang W, et al. A smart copper(II)-responsive binuclear gadolinium(III) complex-based magnetic resonance imaging contrast agent. *RSC Adv* 2014;**4**:34421–7.
- Regueiro-Figueroa M, Gündüz S, Patinec V, Logothetis NK, Esteban-Gómez D, Tripier R, et al. Gd³⁺-based magnetic resonance imaging contrast agent responsive to Zn²⁺. *Inorg Chem* 2015;**54**:10342–50.
- Gianolio E, Porto S, Napolitano R, Baroni S, Giovenzana GB, Aime S. Relaxometric investigations and MRI evaluation of a liposome-loaded pH-responsive gadolinium(III) complex. *Inorg Chem* 2012;**51**:7210–7.
- Bhuiyan MPI, Aryal MP, Janic B, Karki K, Varma NR, Ewing JR, et al. Concentration-independent MRI of pH with a dendrimer-based pH-responsive nanoprobe. *Contrast Media Mol Imaging* 2015;**10**:481–6.
- de Smet M, Langereis S, van den Bosch S, Grüll H. Temperature-sensitive liposomes for doxorubicin delivery under MRI guidance. *J Control Release* 2010;**143**:120–7.
- Bryant DW, McCalla DR, Leeksa M, Laneville P. Type I nitroreductases of *Escherichia coli*. *Can J Microbiol* 1981;**27**:81–6.
- Kitamura S, Narai N, Tatsumi K. Studies on bacterial nitroreductases. Enzymes involved in reduction of aromatic nitro compounds in *Escherichia coli*. *J Pharmacobiodyn* 1983;**6**:18–24.
- Bryant C, Deluca M. Purification and characterization of an oxygen-insensitive NAD(P)H nitroreductase from *Enterobacter cloacae*. *J Biol Chem* 1991;**266**:4119–25.
- Spain JC. Biodegradation of nitroaromatic compounds. *Annu Rev Microbiol* 1995;**49**:523–55.
- Roldán MD, Pérez-Reinado E, Castillo F, Moreno-Vivián C. Reduction of polynitroaromatic compounds: the bacterial nitroreductases. *FEMS Microbiol Rev* 2008;**32**:474–500.
- Chung KT, Murdock CA, Zhou Jr Y, Stevens SE, Li YS, Wei CI, et al. Effects of the nitro-group on the mutagenicity and toxicity of some benzamines. *Environ Mol Mutagen* 1996;**27**:67–74.
- Li Z, Gao X, Shi W, Li X, Ma H. 7-((5-Nitrothiophen-2-yl)methoxy)-3H-phenoxazin-3-one as a spectroscopic off-on probe for highly sensitive and selective detection of nitroreductase. *Chem Commun* 2013;**49**:5859–61.
- Xu J, Sun S, Li Q, Yue Y, Li Y, Shao S. A rapid response “turn-on” fluorescent probe for nitroreductase detection and its application in hypoxic tumor cell imaging. *Analyst* 2015;**140**:574–81.
- Shi Y, Zhang S, Zhang X. A novel near-infrared fluorescent probe for selectively sensing nitroreductase (NTR) in an aqueous medium. *Analyst* 2013;**138**:1952–5.
- Wong RHF, Kwong T, Yau KH, Au-Yeung HY. Real time detection of live microbes using a highly sensitive bioluminescent nitroreductase probe. *Chem Commun* 2015;**51**:4440–2.
- Xue C, Lei Y, Zhang S, Sha Y. A cyanine-derived “turn-on” fluorescent probe for imaging nitroreductase in hypoxic tumor cells. *Anal Methods* 2015;**7**:10125–8.
- Zhu D, Xue L, Li G, Jiang H. A highly sensitive near-infrared ratiometric fluorescent probe for detecting nitroreductase and cellular imaging. *Sens Actuators B: Chem* 2016;**222**:419–24.
- Iwaki S, Hanaoka K, Piao W, Komatsu T, Ueno T, Terai T, et al. Development of hypoxia-sensitive Gd³⁺-based MRI contrast agents. *Bioorg Med Chem Lett* 2012;**22**:2798–802.
- Do QN, Ratnakar JS, Kovács Z, Sherry AD. Redox- and hypoxia-responsive MRI contrast agents. *ChemMedChem* 2014;**9**:1116–29.
- Yang Y, Aloysius H, Inoyama D, et al. Enzyme-mediated hydrolytic activation of prodrugs. *Acta Pharm Sin B* 2011;**1**:143–59.
- Hu L, Fawcett JP, Gu J. Protein target discovery of drug and its reactive intermediate metabolite by using proteomic strategy. *Acta Pharm Sin B* 2012;**2**:126–36.
- Solyanikova IP, Baskunov BP, Baboshin MA, Saralov AI, Golovleva LA. Detoxification of high concentrations of trinitrotoluene by bacteria. *Appl Biochem Microbiol* 2012;**48**:21–7.
- Aime S, Gianolio E, Terreno E, Giovenzana GB, Pagliarini R, Sisti M, et al. Ternary Gd(III)L-HSA adducts: evidence for the replacement of inner-sphere water molecules by coordinating groups of the protein. Implications for the design of contrast agents for MRI. *J Biol Inorg Chem* 2000;**5**:488–97.
- Dickins RS, Aime S, Batsanov AS, Beeby A, Botta M, Bruce JI, et al. Structural, luminescence, and NMR studies of the reversible binding of acetate, lactate, citrate, and selected amino acids to chiral diaqua ytterbium, gadolinium, and europium complexes. *J Am Chem Soc* 2002;**124**:12697–705.